InAsSb detectors for visible to MWIR high operating temperature applications

Citation: D'Souza,A. I., A. C. Ionescu, M. Salcido, E. Robinson, L. C. Dawson, D. L. Okerlund, T. J. de Lyon, R. D. Rajavel, H. Sharifi, D. Yap, M. L. Beliciu, S. Mehta, W. Dai, G. Chen, N. Dhar and P. Wijewarnasuriya. "InAsSb detectors for visible to MWIR high-operating temperature applications", In Infrared Technology and Applications XXXVII, edited by Bjørn F. Andresen; Gabor F. Fulop; Paul R. Norton, Orlando, Florida, USA, April 25, 2011. 80122S. (SPIE Proceedings; vol. 8012). © 2011 SPIE.

As Published: http://dx.doi.org/10.1117/12.884550

Publisher: SPIE--the International Society for Optical Engineering

Persistent URL: http://hdl.handle.net/1721.1/78675

Version: Final published version: final published article, as it appeared in a journal, conference proceedings, or other formally published context

InAsSb detectors for visible to MWIR high operating temperature applications

A. I. D'Souza, A. C. Ionescu, M. Salcido, E. Robinson, L.C. Dawson, D. L. Okerlund
DRS Sensors & Targeting Systems, 10600 Valley View Street, Cypress, CA 90630

T. J. de Lyon, R. D. Rajavel, H. Sharifi, D. Yap, M.L. Beliciu, S. Mehta
HRL Laboratories, LLC, 3011 Malibu Canyon Rd., Malibu, CA 90265

W. Dai, G. Chen
Massachusetts Institute of Technology, Cambridge, MA 02139

N. Dhar
DARPA, MTO, 3701 N. Fairfax Dr., Arlington, VA 22203

P. Wijewarnasuriya
U.S. Army Research Laboratory, 2800 Powder Mill Road, Adelphi, MD 20783

Abstract

The Photon-Trap Structures for Quantum Advanced Detectors (PT-SQUAD) program requires MWIR detectors at 200 K. One of the ambitious requirements is to obtain high (> 80 %) quantum efficiency over the visible to MWIR spectral range while maintaining high D* (> 1.0 x 10^{11} cm √Hz/W) in the MWIR. A prime method to accomplish the goals is by reducing dark diffusion current in the detector via reducing the volume fill ratio (VFR) of the detector while optimizing absorption. Electromagnetic simulations show that an innovative architecture using pyramids as photon trapping structures provide a photon trapping mechanism by refractive-index-matching at the tapered air/semiconductor interface, thus minimizing the reflection and maximizing absorption to > 90 % over the entire visible to MWIR spectral range. InAsSb with bandgap appropriate to obtaining a cutoff wavelength ~ 4.3 μm is chosen as the absorber layer. An added benefit of reducing VFR using pyramids is that no AR-coating is required.

Compound-barrier (CB) detector test structures with alloy composition of the InAsSb absorber layer adjusted to achieve 200 K cutoff wavelength of 4.3 μm (InAsSb lattice-matched to GaSb). Dark current density at 200 K is in the low 10^{-4} A/cm^2 at V_d = -1.0 V. External QE ~ 0.65 has been measured for detectors with a Si carrier wafer attached. Since illumination is through the Si carrier wafer that has a reflectance of ~ 30 %, this results in an internal QE > 0.9.

1.0 Introduction

Infrared detector material is generally grown epitaxially on thick substrates and the radiation is incident on the detector absorber layer through the substrate. Occasionally the substrate is removed and the radiation is incident on the passivated absorber layer. In either case, the refractive index mismatch between the incident medium and the detector or substrate material results in greater than 20 % of the radiation being reflected at the air/detector interface. Multilayer anti-reflection (AR) coatings reduce the reflection down to a few percent when the AR coating is designed for a narrow (~ 0.5 μm in the MWIR) or moderate (3 – 4.3 μm) width spectral band. It is extremely difficult, if not near impossible, to provide an adequate multilayer AR coating with low reflectance across the entire band when the spectral band to be AR coated spans an order of magnitude, 0.5 μm to 4.3 μm in this case.

Infrared Technology and Applications XXXVII, edited by Bjørn F. Andresen, Gabor F. Fulop, Paul R. Norton,
Proc. of SPIE Vol. 8012, 80122S · © 2011 SPIE · CCC code: 0277-786X/11/$18 · doi: 10.1117/12.884550

Tapered nanostructure arrays provide an alternative to multilayer AR-coatings with the added benefit of having broadband reduced reflection.[1-3] Nanostructure arrays with the appropriate geometric shape and dimensions act as photon-trap structures increasing absorption in the detector absorber material. Reduction in absorber volume due to having nanostructures as compared to a single thick absorber layer provides another benefit of reducing the bulk absorber volume, hence reducing the diffusion current from the absorber material. Optimization of the geometric nanostructure shape to reduce broadband reflection, increase broadband absorption while reducing bulk absorber volume results in a high performance photon trap device.

2.0 Geometric Modeling

Broadband high quantum efficiency requires minimizing the reflection of the radiation incident on the detector and maximization of the radiation in the detector absorber material. Due to the high refractive index of the absorber material, the reflection off a flat absorber would be ~ 30 %. In order to attain these objectives, the InAsSb absorber material is contoured to have a pyramidal shape as shown in Figure 1. Radiation incident on an array of pyramids reduces the reflection across a broad spectral band as well as enhance photon trapping in the absorber material.

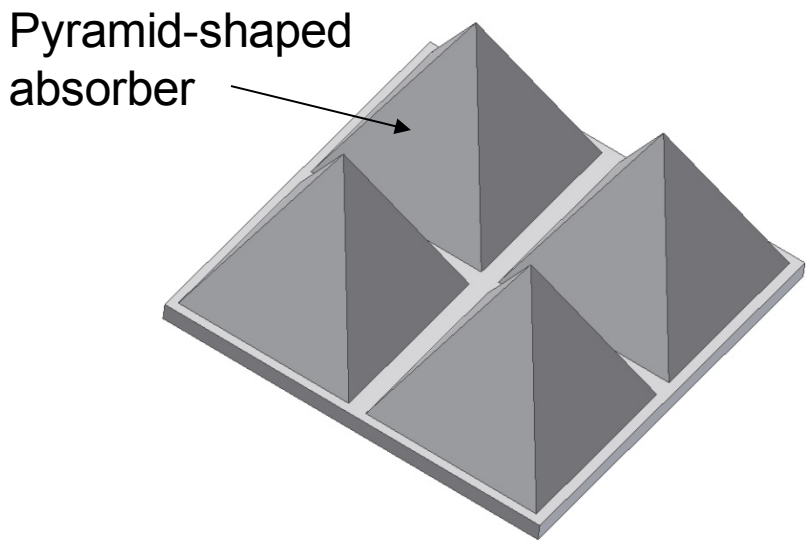

Figure 1. Pyramid shaped absorber to minimize broadband reflection and increase absorption in the InAsSb absorber material

Front-side reflectance is reduced by using geometric shapes and dimensions that increase the coupling of the incident light into the absorber material and also that increase the scattering of the in-coupled light. These structural features have a greater influence on the reflection of the shorter-wavelength light. A reduced front-side reflection is also beneficial for suppressing spectral peaks and notches associated with optical-cavity resonances.

Simulations were done using two different frequency-domain, finite-element analysis tools as well as a finite-difference time-domain analysis tool, all of which provided consistent results. The simulations indicate that the pyramidal contoured detector can achieve high absorbance (with > 98% absorption) of the incident light over the full wavelength range extending from 0.5 μm to 5.0 μm as shown in figure 2. Simulations also suggest that intentional misalignment of the pyramid array pattern is helpful for avoiding

deep drops in the absorbance spectrum. The high absorbance indicates that the reflectance is low (< 2%) for the broad 0.5 μm to 5.0 μm spectral band for the misaligned array case. For the simulation results displayed in figure 2, the total volume of the pyramidal absorber is equivalent to a uniform-height bulk absorber layer with a thickness of 2.53 μm, which defines a parameter called the "effective absorber thickness" for the detector. In order to establish the efficacy of the pyramid shaped absorber to reduce bulk diffusion current, it is necessary to determine the volume of bulk absorber that is equivalent in absorbance and reflectance to the pyramid shaped absorber. In comparison to the effective thickness of 2.53 μm for the detector simulated, a single-pass absorbing layer of uniform height would need to have a thickness of at least 12 μm and also need to have a perfect anti-reflection coating, resulting in an absorber volume reduction of 4.74X while maintaining absorbance in the InAsSb material.

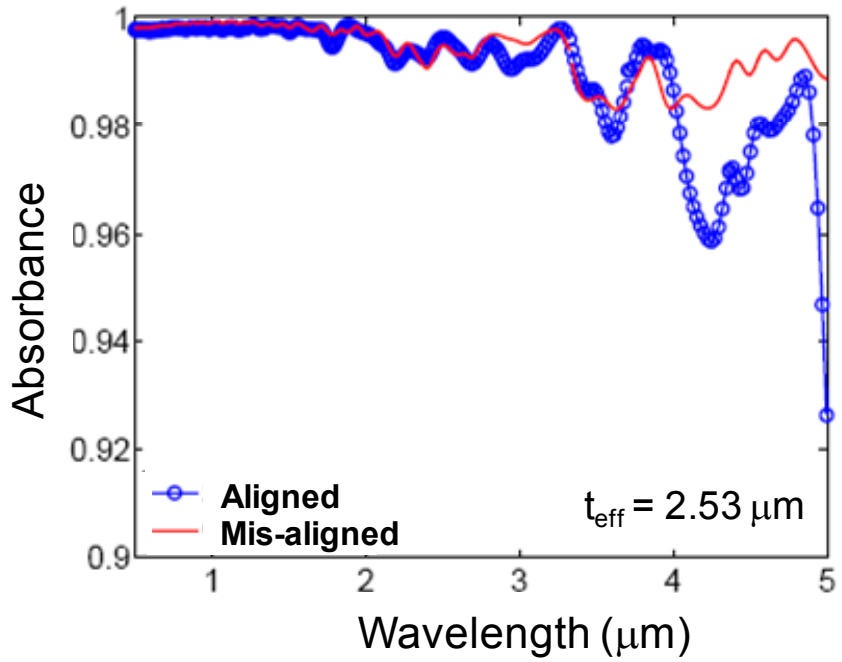

Figure 2. Absorbance as a function of wavelength for the pyramid shaped InAsSb absorber

3.0 Detector Architecture

Innovative nBn barrier detectors[4] have been designed to suppress majority carrier current while maintaining a low electric field. This nBn design was considered a remedy to the generation-recombination currents originating in the depletion region of p-n junction devices. However, the original InAsSb/AlAsSb barrier device design can have potential deficiencies associated with the choice of AlAsSb as the barrier material, including difficulties in controlling the barrier electrical conductivity with substitutional doping and chemical instability of the AlAsSb.[5] Circumventing some of the difficulties resident in the original nBn design, a compound-barrier (CB) detector architecture was designed and implemented with alloy composition of the InAsSb absorber layer adjusted to achieve 200K cutoff wavelengths of 4.3 μm.[5] The novel detector structure which is displayed in figure 3 utilizes pyramid-shaped absorbers. Each detector pixel has an array of multiple pyramid-shaped absorbers. This detector structure provides the combination of reduced volume of absorber material, elimination of front-side reflection for incident light over a broad bandwidth, and enhanced photon trapping for high absorbance of that incident light.

Infrared radiation is incident on the array of pyramids fabricated in the n-type InAsSb absorber which also serves as the array common or substrate contact. The detector array is hybridized via Indium bumps to a Si fanout chip. The Si fanout chip when inserted into an 84 pin leadless chip carrier (LCC) permits direct access to the two terminals of ~ 80 detectors.

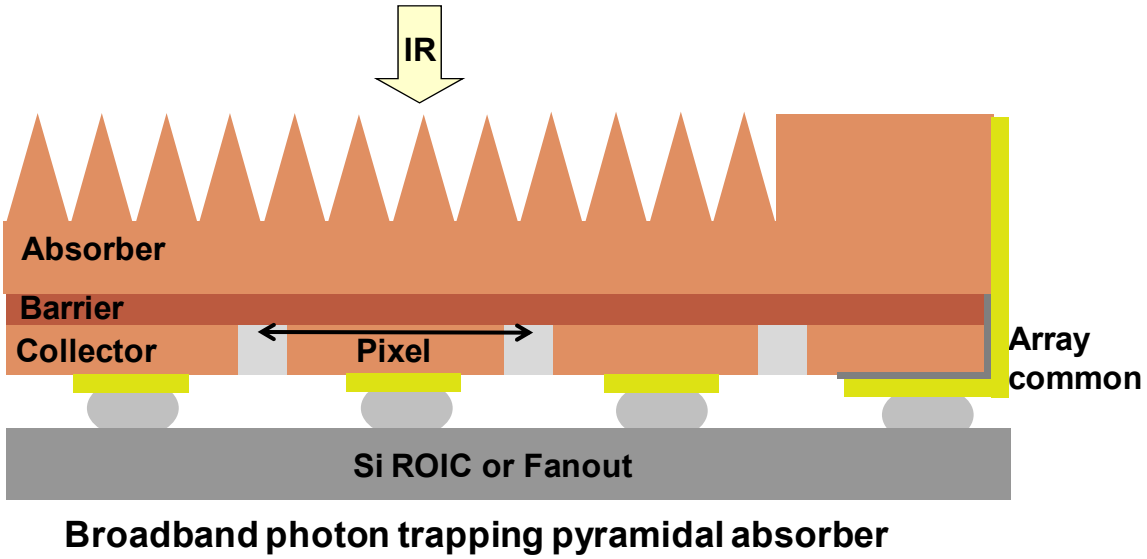

Figure 3. Compound barrier detector architecture with pyramid shaped absorber layer

4.0 Array Processing

The detector is an InAsSb-based barrier device which uses robust III-V processing capability for the fabrication of detector arrays with photon trapping characteristics. The architecture utilizes a backside process for contacting the array common and the individual pixels to the Si fanout chip. This architecture which utilizes complete substrate removal eliminates the need for front side contacts and any associated parasitic reflection losses. Figure 4 is an SEM picture of pyramids fabricated in an InAsSb epilayer.

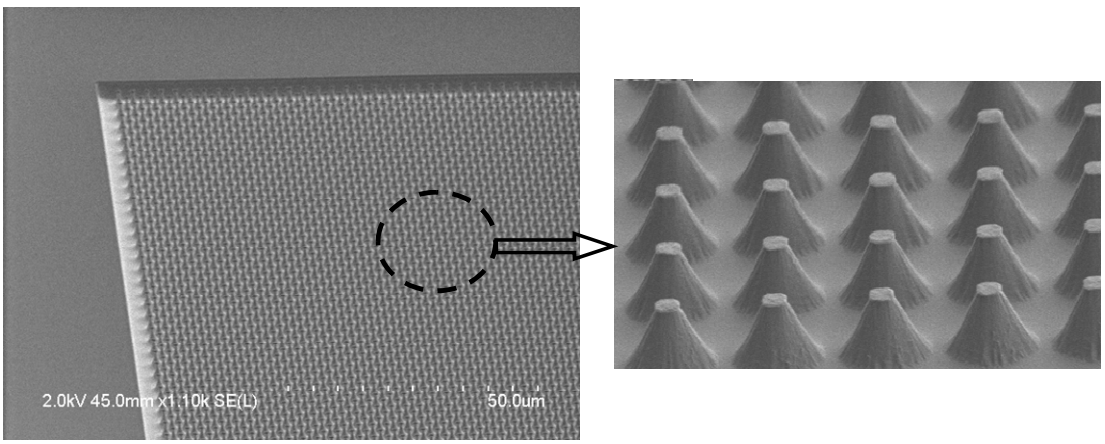

Figure 4. SEM image of the pyramidal photon trapping absorber on a layer of InAsSb epilayer.

5.0 Detector and Array Data

128 x 128 detector arrays are hybridized to Si fanout chips. The Si fanout permits access to the two terminals of individual detectors permitting easy acquisition of I-V data under dark and illuminated conditions. Figure 5 is a plot of the dark current density as a function of temperature for a 4.3 μm cutoff wavelength detector. Dark current density at 200 K is ~ 1.3 x 10^{-4} A/cm^2. A switching matrix permits multiple J_d – V measurements without intervention. Photocurrent versus bias is also measured at 200 K. From the photo and dark current at 200 K, the quantum efficiency (QE) versus bias is calculated and plotted in Figure 6. As can be seen from figure 6, a bias in the 800 mV range is required before the QE approaches its maximum value. The external QE is 0.67. Since the Si carrier wafer is still attached to the detector, the maximum QE possible is ~ 0.7, therefore the internal QE ~ 0.96 is close to the value predicted from the absorption modeling. There exists an unintentional barrier introduced during processing. Origin of the barrier introduced during processing is unknown, but modifications to the processing sequence resulted in elimination of the additional barrier. Shown in Figure 7 is a normalized response versus bias which shows detectors manufactured using a modified processing sequence showing detector response saturating at ~ 100 mV. This proves that the steps in the processing sequence that resulted in an additional unintended barrier have been eliminated for detectors manufactured using the modified process.

Dark current density at -1.0 V is plotted as a function of temperature in Figure 8. An exponential least squares fit reveals the calculated activation energy for the detector to be E_a = 333.4 meV. The equation for $InAs_{1-x}Sb_x$ bandgap[6,7] $E_g(x,T)$ is shown in equation 1. For x = 0.09 (the value used to lattice match $InAs_{1-x}Sb_x$ to the GaSb substrate) and T = 0 K, the value of E_g is 338 meV, close to the activation extracted from the dark current density versus temperature data, indicating that the dark current density at -1.0 V is dominated by diffusion current.

$$E_g(x,T) = 0.411 - \frac{3.4\times10^{-4}T^2}{210+T} - 0.876x + 0.70x^2 + 3.4\times10^{-4}xT(1-x) \text{ ---------- (1)}$$

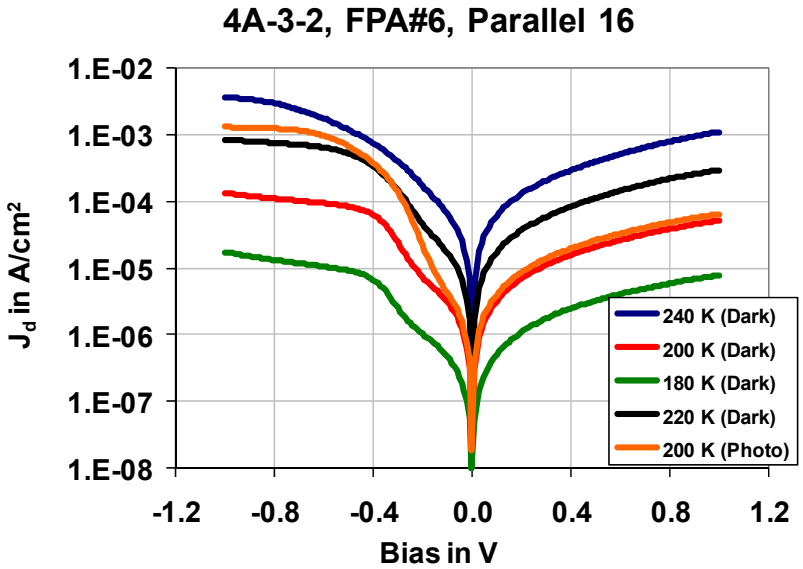

Figure 5. Dark current density J_d versus bias and temperature for sample barrier detector. Dark and illuminated J_d at 200 K.

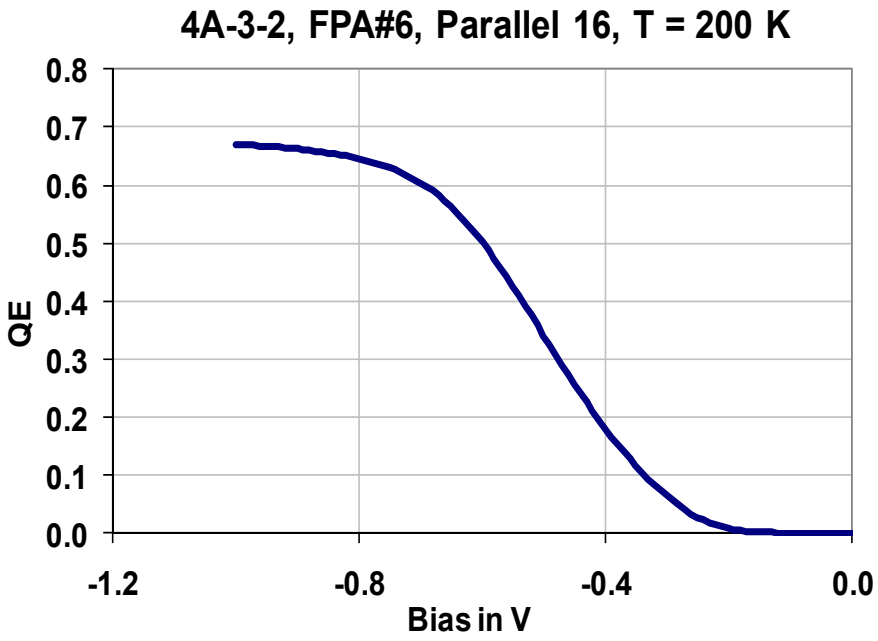

Figure 6. Quantum efficiency versus bias at 200 K calculated from the J – V curves shown in Figure 5.

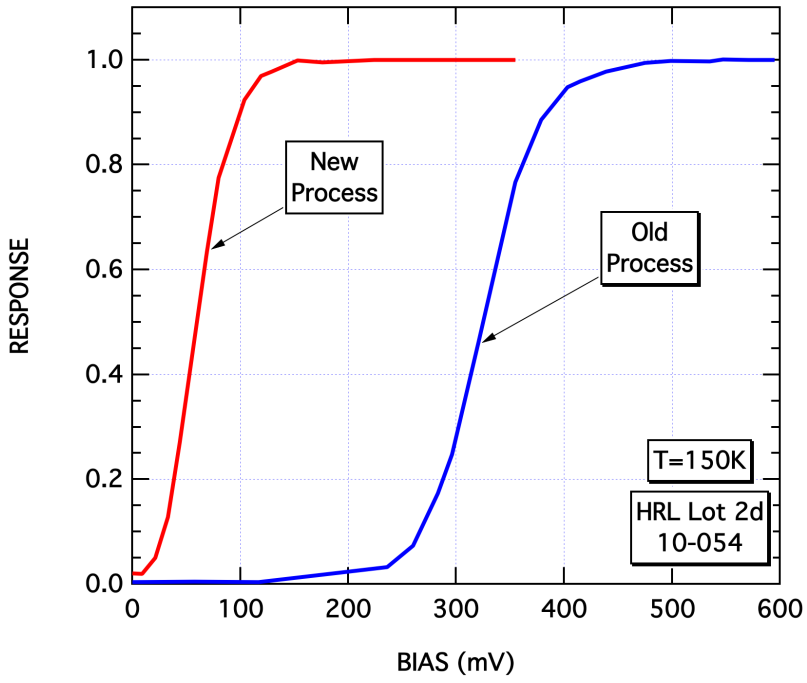

Figure 7. Normalized response versus bias for detectors manufactured in an initial lot and following a modified processing sequence

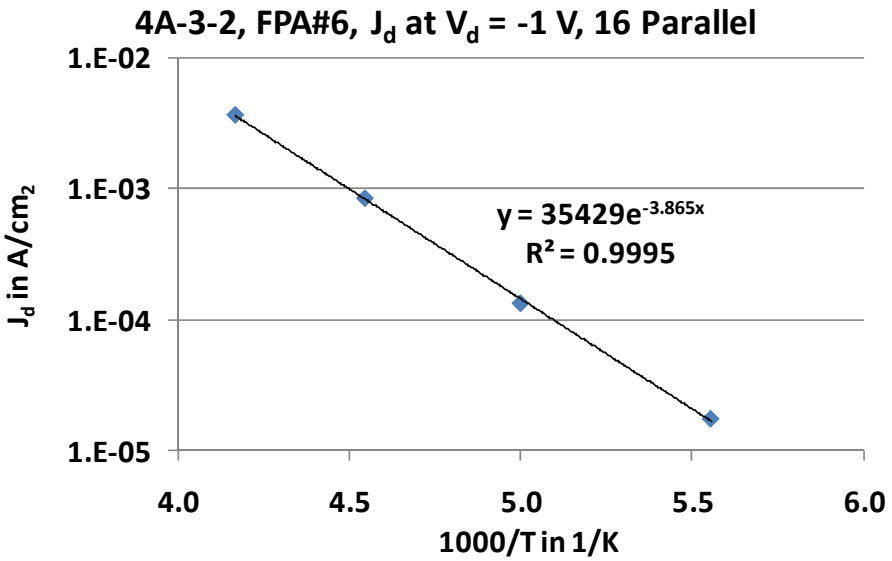

Figure 8. Activation energy extracted from dark current density versus temperature at -1.0 V

Spectral response for a barrier detector (different from the one measured and displayed in Figures 5, 6 and 8) with $InAs_{1-x}Sb_x$ (x = 0.09) as the active layer is displayed in Figure 9. A Nicolet Fourier Transform Infrared (FTIR) Spectrometer is used to measure the spectral response at wavelengths from 1.6 μm to 5.0 μm. A monochromator is used to measure response from the visible 0.5 μm to the near infrared 1.04 μm. Source of the radiation is a light bulb that illuminates a diffraction grating. A Newport Visible/UV detector with known quantum efficiency between 200 nm to 1.1 μm is used to calibrate the flux as a function of wavelength emanating from the monochromator. Photocurrent from the $InAs_{1-x}Sb_x$ detector is divided by the calibrated flux, area of the $InAs_{1-x}Sb_x$ detector and charge of the electron to determine quantum efficiency as a function of wavelength. Placement of the $InAs_{1-x}Sb_x$ detector at any location other than the location of the calibrated detector results in flux errors with consequential quantum efficiency errors.

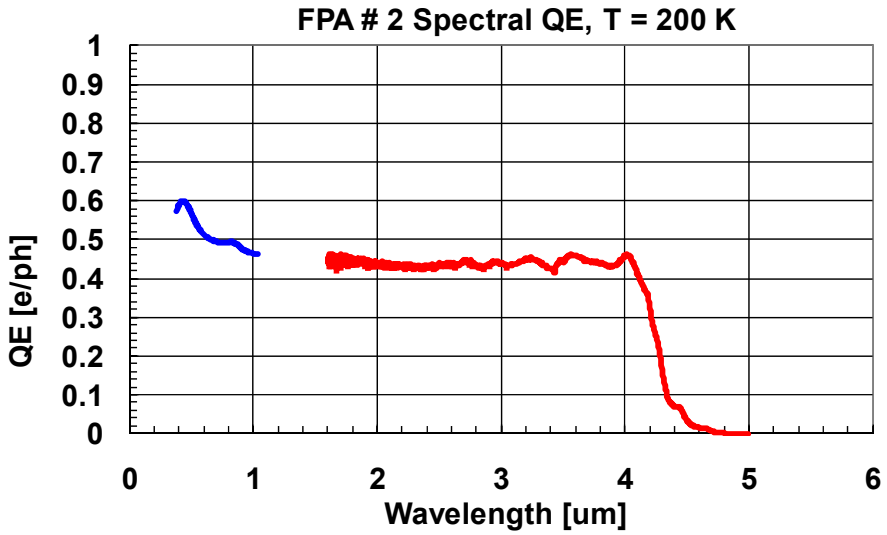

Figure 9. Quantum Efficiency versus wavelength

6.0 Summary and Conclusions

The photon trap pyramidal absorber has been designed to provide a combination of reduced volume of absorber material, elimination of front-side reflection for incident light over a broad bandwidth, and enhanced photon trapping for high absorbance of that incident light. Geometric modeling of the absorber determined the pyramid shape to maximize absorption and minimize reflectance over the broad wavelength range of 0.5 μm to 5.0 μm. Barrier detectors measured showed diffusion limited performance at a 1 V bias. Detectors showed response from 0.5 μm to the 4.3 μm detector cutoff and the internal quantum efficiency is in the 90% range.

7.0 Acknowledgements

This work was supported by DARPA under contract N66604-09-C-3652 (Nibir Dhar, DARPA Program Manager). Special thanks to Dr. Ravi Dat, Booz Allen Hamilton for technical and other advice. Excellent work was performed by Prof. Saif Islam and his team at UC Davis who were instrumental in different aspects of the processing sequence.

8.0 References

1. J. Zhu, Z. Yu, G.F. Burkhard, C-M Hsu, S.T. Connor, Y. Xu, Q. Wang, M. McGehee, S. Fan, Y. Cui, *Nano Lett.*, **2009**, *9* (1), pp 279–282.
2. L. Hu, G. Chen, *Nano Lett.*, **2007**, *7* (11), pp 3249–3252.
3. Y-J. Lee, D.S. Ruby, D.W. Peters, B.B. McKenzie, J.W.P. Hsu, *Nano Lett.*, **2008**, *8* (5), pp 1501–1505.
4. White, Anthony M., USA Patent No. 4,679,063 (1987).
5. T. de Lyon, R. Rajavel, H. Sharifi, M. Beliciu, S. Terterian, M. Roebuck, D. Yap, A. D'Souza, A. Ionescu, D. Okerlund, P. Wijewarnasuriya, To be published in 2011 MSS Detector Specialty Group Meeting Proceedings.
6. Antoni Rogalski, "Infrared Photon Detectors", SPIE Optical Engineering Press, Bellingham, Washington, USA, p 352.
7. H.H. Wieder, A.R. Clawson, *Thin Solid Films* 15, 217 (1973).